Investigation of new nondegenerate dual-mode microstrip patch filter

A.F. Sheta, N. Dib and A. Mohra

Abstract: A new nondegenerate dual-mode microstrip patch filter structure is introduced. The proposed filter is based on a square microstrip patch with four slots etched in symmetrical form. Besides its simple structure, the filter has the advantages of small size and low loss. The full-wave IE3D package is used to analyse the proposed structure. Design curves that relate the mode resonance frequencies and fractional bandwidth against slot parameters are presented. A bandpass filter is designed, analysed and tested at 2.15 GHz. Experimental results show good agreement with theoretical results.

1 Introduction

The use of planar dual-mode resonators for bandpass filter applications was first proposed by Wolff [1]. Dual-mode microstrip resonators are attractive because each resonator can be used as a doubly tuned circuit and, therefore, the number of resonators required for a given degree of filter is reduced by half. Various types of dual-mode microstrip line resonators have been proposed [1–6]. The bandpass filter response has been obtained through: (i) the excitation of the two degenerate modes by asymmetrical feed lines and (ii) adjusting the coupling between the two modes by adding suitable form of perturbation within the resonators. Although these line resonators are smaller in size than the patch dual-mode resonators, they suffer from higher conductor loss and lower power-handling capability. For these reasons, various forms of dual-mode microstrip patch resonators have been proposed to design bandpass filters for low loss and high power-handling capability [7–10]. The resonators can take different forms such as circular, square and triangular patch [7–9]. The coupling between the degenerate modes is also adjusted by using appropriate perturbation in the patch resonators. Crossed slotted square patch [10] and circular patch with etched holes [11] have been proposed for both size and loss reduction. Comparison based on experimental results [12] shows that the unloaded quality factor of the covered microstrip line resonators, such as ring and square loop, are slightly lower than the microstrip disc and square patch.

In this paper, a dual-mode square-patch resonator, with four slots etched in symmetrical shape, is proposed for small-size and low-loss bandpass filter applications. More than 70% area saving with respect to the conventional dual-mode square patch is possible. In contrast to the conventional degenerate mode filters, which are usually used for narrowband (less than 5% fractional bandwidth) applications, the proposed filter can be designed for fractional bandwidth from about 5% to more than 25%. Asymmetrical feed lines are used to excite the degenerate modes and the first higher-order mode. The analysis is carried out using the full-wave IE3D package.

In the following Section, the modes of conventional square patch as well as the effect of the feeding structure on the excited modes are described.

2 Mode resonance frequencies and excitation mechanism of a square patch

The square patch resonator can be considered as a square cavity with magnetic walls. The field inside the cavity corresponds to those of TM^{z}_{mn0} modes [8]. The resonance frequencies of these modes can be calculated from [13]. Duroid substrate with $\varepsilon_r = 10.2$ and thickness of 0.635 mm is used in this paper. For a square of length 17 mm, the resonance frequency of the first two orthogonal modes, TM_{100} and TM_{010}, calculated from [13], is $f_{100} = f_{010} = 2.76$ GHz. The resonance frequency of the TM_{110} mode is $f_{110} = 4.02$ GHz.

Generally speaking, the excited modes depend on the feeding structure [14]. This can be easily observed from the current distribution, calculated from the IE3D simulator, on the patch as shown in Fig. 1. For centred symmetric feed lines, the only excited mode is the TM_{100} if the feed lines are along the X-axis (Fig. 1*a*), while the TM_{010} mode is excited if the feed lines are along the Y-axis (Fig. 1*b*). The TM_{110} mode is not excited if any of the feed lines are located at the centre of the vertical or horizontal edge. For asymmetric nonorthogonal excitation, such as the case shown in Figs. 1*c* and 1*d*, the two modes, TM_{100} and TM_{010}, are excited simultaneously with the TM_{110} mode. Figure 1*c* shows the current distribution of the two modes TM_{100} and TM_{010} at 2.76 GHz, while Fig. 1*d* shows the current distribution corresponding to the TM_{110} mode at 4.02 GHz.

3 Slotted square patch analysis

The element structure that represents the main building block of the proposed filter is a square patch with four

IEE Proceedings online no. 20050103

doi:10.1049/ip-map:20050103

Paper first received 5th May and in revised form 8th September 2005

A.F. Sheta is with the Electrical Engineering Department, King Saud University, P.O. Box 800, Riyadh 11421, Saudi Arabia

N. Dib is with the Electrical Engineering Department, Jordan University of Science and Technology, Irbid, Jordan

A. Mohra is with the Microstrip Department, Electronics Research Institute, Cairo, Egypt

E-mail: nihad@just.edu.jo

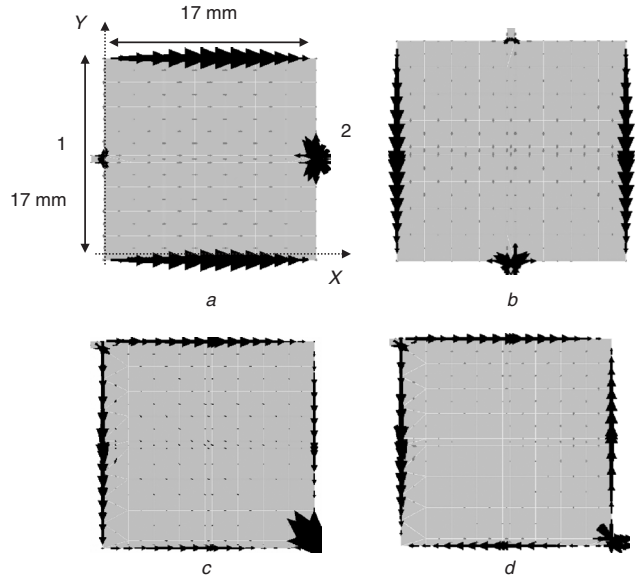

Fig. 1 *Current distribution of first three modes of square patch of side length of 17 mm on Duroid substrate with $\varepsilon_r = 10.2$ and thickness 0.635 mm*
a Current distribution of TM_{100} mode at 2.76 GHz
b Current distribution of TM_{010} mode at 2.76 GHz
c Current distribution of two modes TM_{100} and TM_{010} at 2.76 GHz
d Current distribution of TM_{110} mode at 4.02 GHz

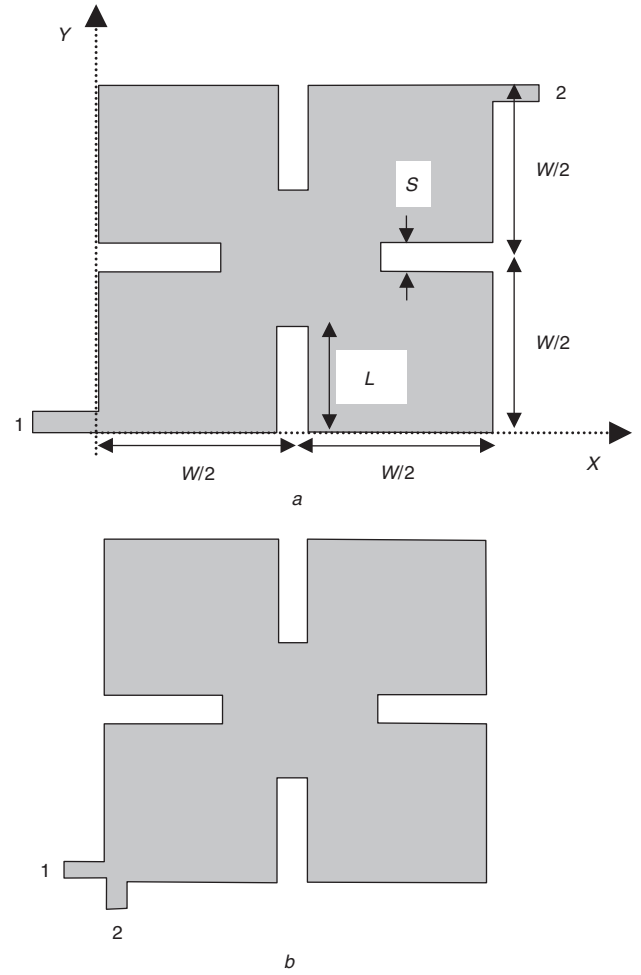

Fig. 2 *Dual-mode bandpass filter*
a Proposed nondegenerate dual-mode filter element
b Asymmetric feed lines to simultaneously excite the TM_{100}, TM_{010}, and TM_{110} modes

symmetrically etched slots as shown in Fig. 2*a*. The square patch has a length W, while the slots have equal lengths L and width S. The resultant modes can now be considered as perturbed types of that of the unslotted square patch described in Section 2. It has first to be noted that introducing slots normal to the current path will simply increase the effective length of the resonator. Hence, it is expected that the resonance frequencies of all modes having nonzero current at the centre of the patch, normal to the slots, will decrease as the length L of the slots increases. However, all modes having zero current at the centre, such as the TM_{200} mode, will be almost unaffected. The vertical slots will affect the resonance frequency of the TM_{100} mode, because the current distribution of this mode is parallel to the feed line (in the X-direction). Similarly, horizontal slots have the same effect on the resonance frequency of the TM_{010} mode. Furthermore, the opposite currents on the slot sides will reduce the radiation loss, where the radiation loss decreases as the slot width decreases. However, the TM_{110} mode has currents in both X and Y directions, thus its resonance frequency will be affected by both vertical and horizontal slots. The current turns around the slots, and so reduction in radiation loss from this mode is expected too. As the structure shape is symmetric, the two degenerate modes, TM_{100} and TM_{010}, do not split and will have the same resonance frequency, which will be denoted as f_1. The resonance frequency of the TM_{110} mode will be denoted as f_2. Asymmetric feed-line excitation at one corner of the square patch, as shown in Fig. 2*b*, is proposed to study the influence of the slot parameters (width and length) on the resonance frequencies, f_1 and f_2. This feeding technique excites approximately all possible modes that can be supported by the patch. The feeding structure has been

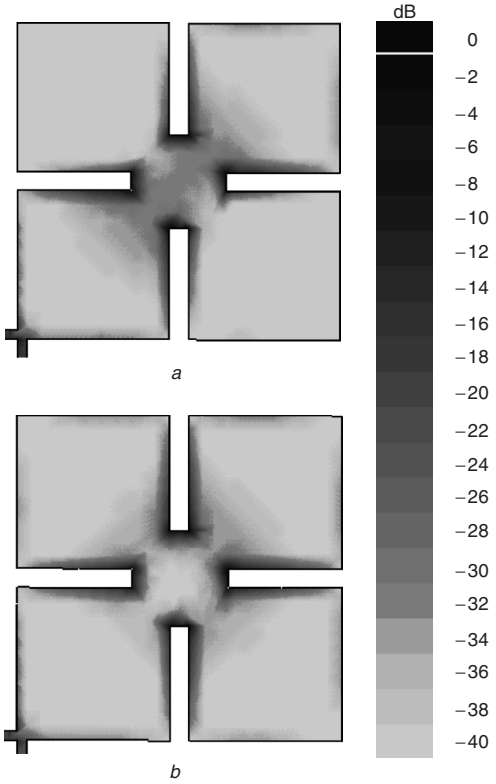

Fig. 3 *Simulated current density of the excited modes for $W = 17$ mm, $L = 6$ mm and $S = 1$ mm*
a The two modes TM_{100} and TM_{010} at their resonance frequency of 1.925 GHz
b The TM_{110} mode at its resonance frequency of 2.25 GHz

validated through the comparison of the first ten excited modes of a square of length 65.33 mm presented in [13]. The IE3D simulator is used in this comparison. The error observed is less than 0.7%. Figures 3*a* and 3*b* show the simulated two-dimensional current density over the whole conductor surface of the three modes for $W = 17$ mm, $L = 6$ mm and $S = 1$ mm. The current density is concentrated around the slots, and significantly at the ends of the slots. Figure 3*a* shows the current density where the two modes TM_{100} and TM_{010} are excited. Very little current appears at the corners and the centre of the patch. Figure 3*b* shows the current density of the TM_{110} mode, where almost no current is observed at the centre and the corners of the patch.

The effect of the length L and width S of the slots on the resonance frequencies is studied based on a patch of $W = 17$ mm on Duroid substrate. The effect of the slot length L, for slot width S of 1 mm, on f_1 and f_2 is shown in Fig. 4*a*. The two resonance frequencies f_1 and f_2 decrease as L increases. However, f_2 decreases faster than f_1, because the TM_{110} mode is affected by both vertical and horizontal slots. Both f_1 and f_2 become close to each other when L increases. For $L = 7.8$ mm, f_1 decreases from 2.76 to 1.44 GHz, while f_2 decreases from 4.02 to 1.55 GHz. Figure 4*b* shows the effect of slot width S on f_1 and f_2 for $L = 6$ mm. As noted in the preceding, as f_2 is affected by both vertical and horizontal slots, it decreases faster than f_1 as S increases. Other curves can be plotted for other combinations of S and L, and, thus, more frequency reduction can be obtained. As an example, for $S = 2$ mm and $L = 7.4$ mm, $f_1 = 1.355$ GHz and $f_2 = 1.41$ GHz.

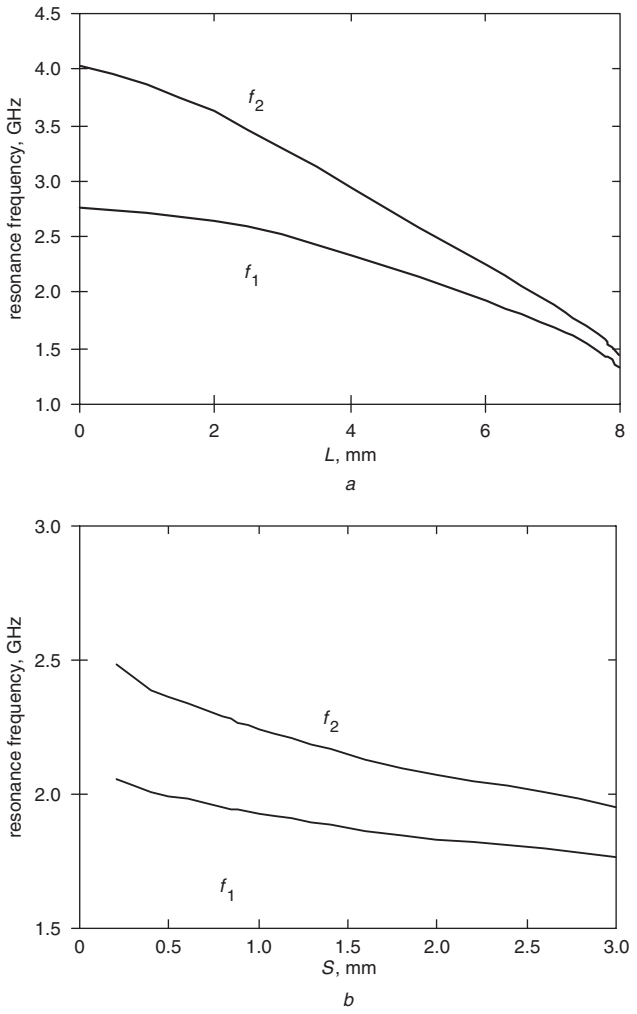

Fig. 4 *Mode resonance frequencies against slot length L and width S of the element of Fig. 2b for W = 17 mm on Duroid substrate with $\varepsilon_r = 10.2$ and thickness 0.635 mm*
a Effect of slot length for slot width $S = 1$ mm
b Effect of slot width for slot length $L = 6$ mm

4 Dual-mode bandpass filter

Now, the design of a bandpass filter is investigated by studying the effect of the slot length and width on a dual-mode resonator filter. Figure 5 shows a group of simulated curves, obtained using the IE3D simulator, of the structure in Fig. 2*a* for different slot lengths. Direct-feed 50 Ω microstrip lines of 1 mm length at the corners, as shown in Fig. 2*a*, are used. It is found that, as L increases, the filter

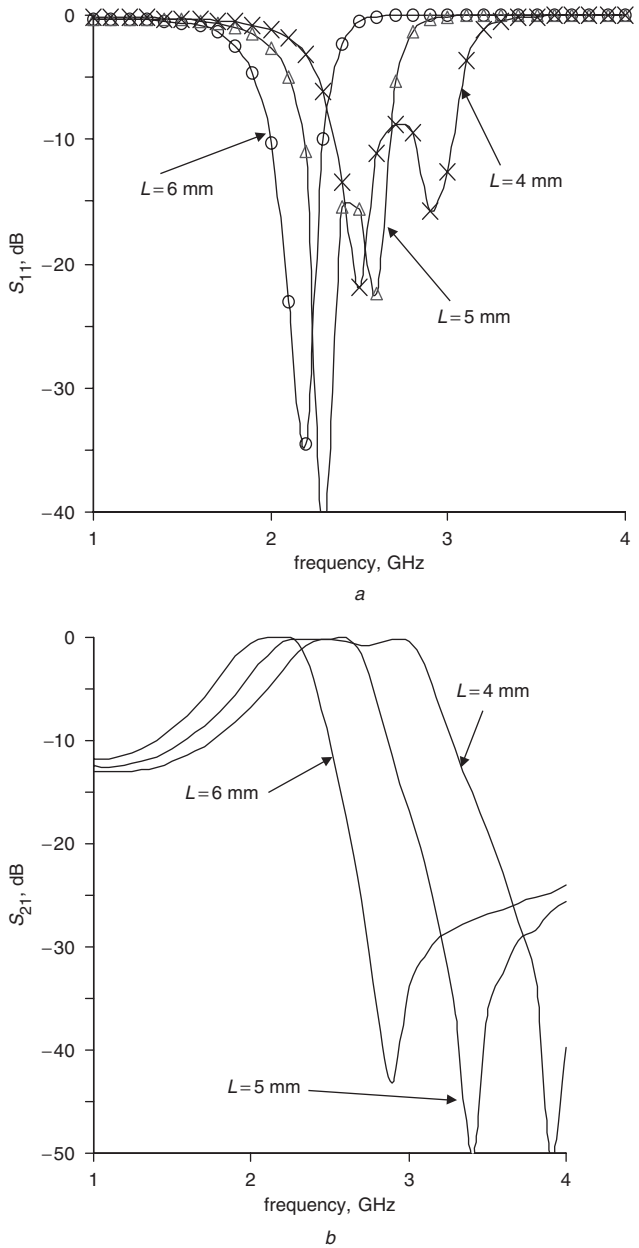

Fig. 5 *Simulated frequency response of dual-mode filtering behaviour for different values of slot length L with S = 1 mm, W = 17 mm, $\varepsilon_r = 10.2$ and h = 0.635 mm*
a Return loss
b Insertion loss

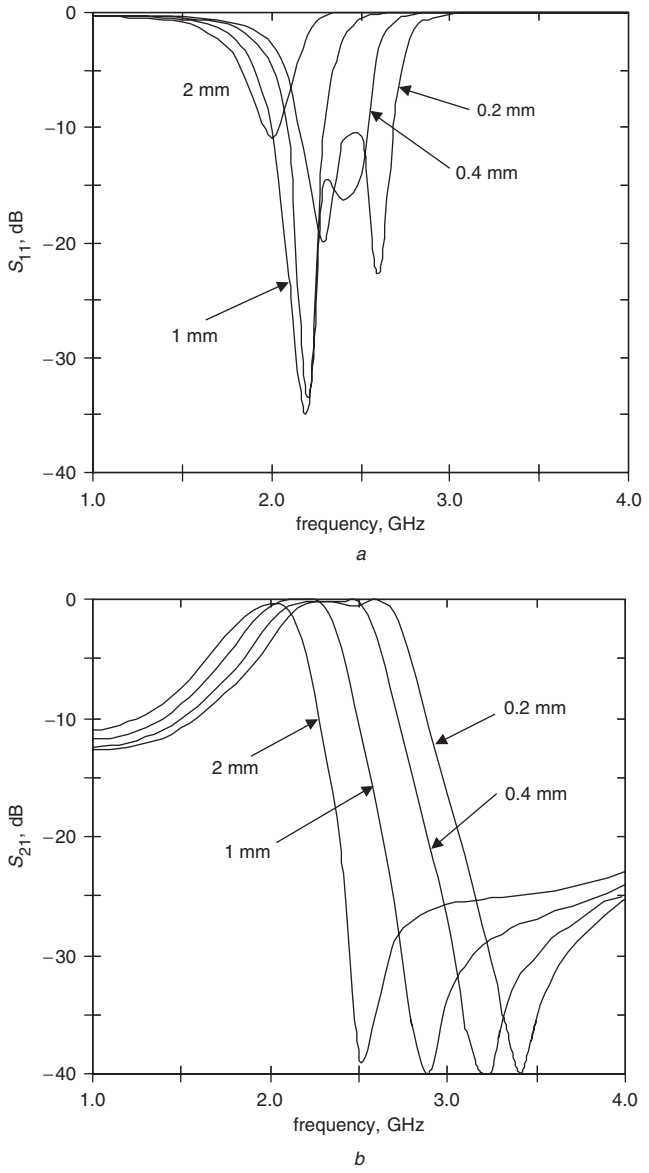

Fig. 6 *Simulated frequency response of dual-mode filtering behaviour for different values of slot width S with L = 6 mm, W = 17 mm, $\varepsilon_r = 10.2$ and h = 0.635 mm*
a Return loss
b Insertion loss

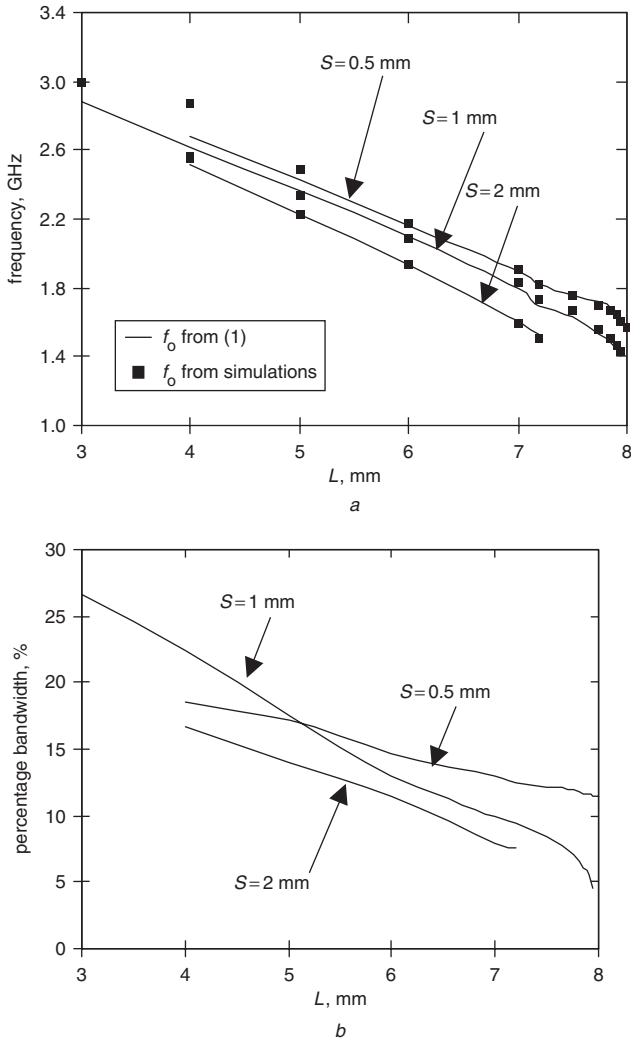

Fig. 7 *Variation of filter resonance frequency (a) and fractional bandwidth (b) against L for different values of S*

behaviour shifts to lower frequencies, and the bandwidth becomes narrower. This confirms, with the conclusion made from Fig. 4, that f_1 and f_2 become close to each other when L increases. Similar observations can be made from Fig. 6 which shows the effect of the slot width on the filter behaviour for $L = 6$ mm. Figures 5*a* and 6*a* show that matching is not always good for all the slots' dimensions, so, in some cases, quarter-wavelength lines might be needed, to improve matching and increase the flexibility, to design the bandpass filter element with a specified performance. The filter centre frequency can be approximated by

$$f_o = \sqrt{f_1 f_2} \quad (1)$$

Figure 7 shows the variation of the filter centre frequency f_o and the fractional bandwidth against L for different values of S. A series of simulations performed by the IE3D simulator is used to obtain these curves. The fractional bandwidth is estimated for S_{11} less than -10 dB, where the simulated centre frequency is the midband frequency. This shows that the centre frequency calculated by (1) is very close to that determined from the IE3D simulator for L greater than 4 mm. This Figure shows also that S does not have significant effect on the filter centre frequency. Fractional bandwidths from about 5% to more than 25% can be obtained for $S = 1$ mm. It has been observed that this range is reduced for $S = 0.5$ mm and 2 mm. These curves show the flexibility of the structure to design a bandpass filter with specified bandwidth. Two design examples are given as follows:

Case 1: This example compares the response of a narrow-band filter based on the slotted patch, proposed in this paper, and that of a conventional cut-corner square patch. The nondegenerate dual-mode filter is designed for 5% fractional bandwidth. The physical parameters are $W = 17$ mm, $L = 7.95$ mm and $S = 1$ mm. The centre frequency is 1.425 GHz. Good matching cannot be obtained by 50 Ω direct feed lines, therefore a 75.6 Ω quarter-wavelength impedance transformer, of 0.18 mm width, is added to improve the matching. The lines are placed 0.5 mm away from the patch and parallel to it to save space. Simulations show that the effect of placing the feeding lines at this distance is not significant and can easily be neglected. For about the same centre frequency, a conventional, cut-corner, 33.5×33.5 mm^2 square patch is designed. The

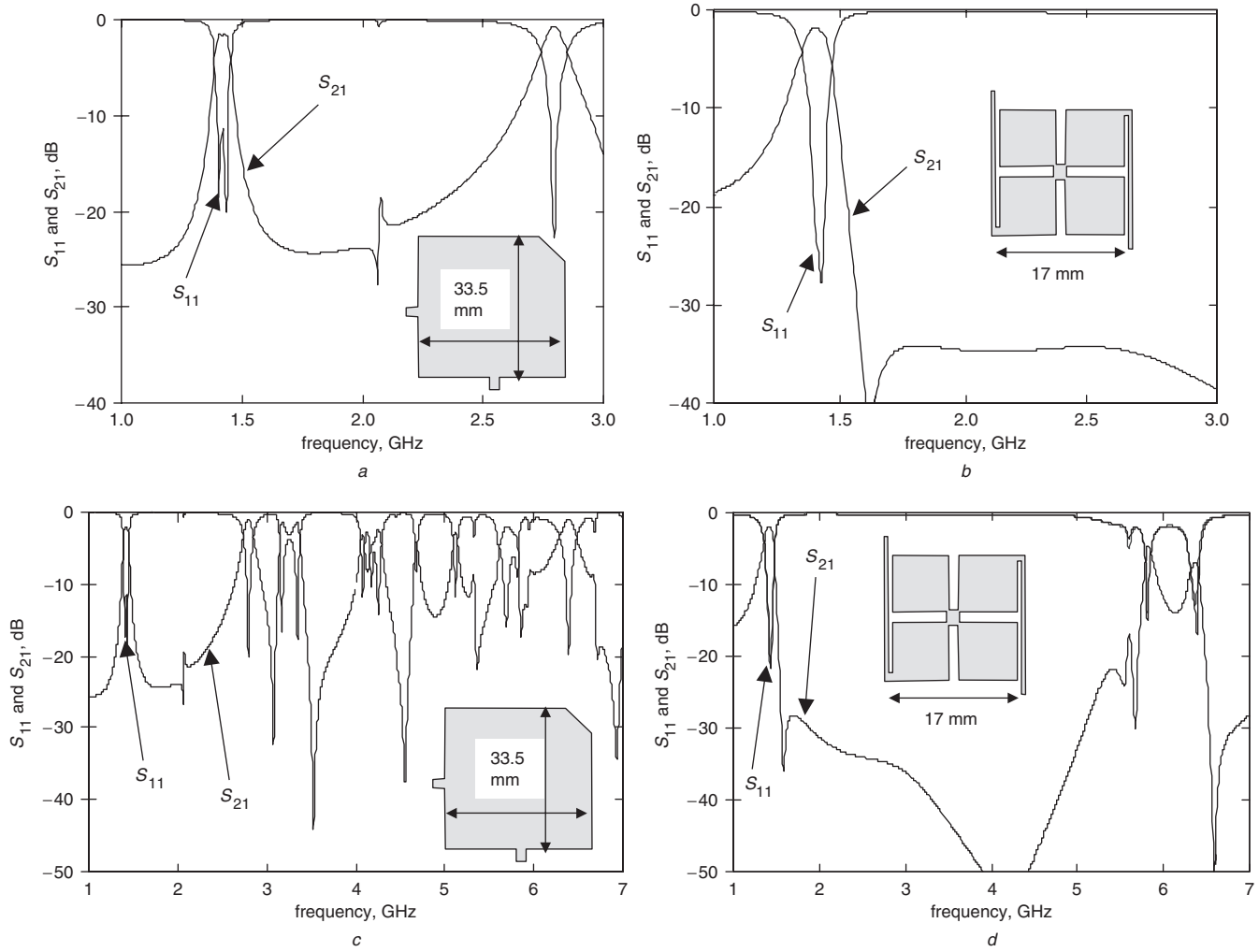

Fig. 8 *Simulation results of two filters: conventional degenerate dual-mode cut-corner 33.5 × 33.5 mm square patch (a, c), and proposed nondegenerate dual-mode 17 × 17 mm filter (b, d), designed at about 1.425 GHz on Duroid substrate with $\varepsilon_r = 10.2$ and thickness 0.635 mm*
a, b Narrowband behaviour
c, d Broadband behaviour to show the spurious response

simulation results of the two filters are shown in Fig. 8. Figures 8*a* and *b* show the narrowband behaviour and Figs. 8*c* and *d* show the broadband characteristics. The obtained fractional bandwidth of the square cut-corner filter is about 3.4% and the minimum insertion loss is 1.6 dB. However, the minimum insertion loss of the proposed filter is 1.9 dB and the relative bandwidth is 5.2%. The patch area used by the proposed structure is about 26% of that of the conventional type. Moreover, in contrast to the conventional type, sharp wide stopband rejection is obtained in the higher band and no harmonic response is observed up to about 5.7 GHz ($3.9f_o$). These advantages are obtained at the expense of 45% reduction of the unloaded quality factor. The unloaded quality factor calculated from the simulation results is 88.

Case 2: In this case, a bandpass filter with wider bandwidth is designed. The selected fractional bandwidth is 13%. The filter physical parameters are $W = 17$ mm, $L = 6$ mm and $S = 1$ mm. Figure 9 shows the simulation and experimental results, from 1 to 10 GHz, of the filter developed on Duroid material with $\varepsilon_r = 10.2$ and thickness 0.635 mm. Good matching is obtained using direct 50 Ω feed lines. Very good agreement between simulated and experimental results is observed, which validates our filter design. The measured filter bandwidth for S_{11} less than −10 dB is 270 MHz centred at 2.12 GHz (∼13%). Within this band the measured insertion loss is -0.6 ± 0.25 dB. The bandwidth obtained in this example is not possible to achieve using conventional cut-corner square patch. Wide stopband characteristics are observed with relatively small out-of-band rejection. Better rejection can be obtained by cascading two or more identical elements. Figure 10 shows the simulations and experimental results of cascaded two identical elements of the filter designed herein. For compactness, a 1 mm separation between the two elements is selected. Experimental results are performed in uncovered condition. A little decrease in bandwidth, from 270 to 230 MHz, is observed. The rejection is approximately doubled in the stopband and the measured insertion in the passband is 1.05 ± 0.45 dB. The unloaded quality factor calculated from the measured results is approximately 170. This value is slightly larger than those reported in [12], where the unloaded quality factors Qu = 167, for a ring resonator, and Qu = 161, for a square loop, were obtained in uncovered environment at about 1.55 GHz, using Duroid substrate with $\varepsilon_r = 10.8$ and thickness of 1.27 mm. It can be noted from these examples that the unloaded quality factor decreases as the filter size is reduced. Photographs of the fabricated filters are shown in Fig. 11.

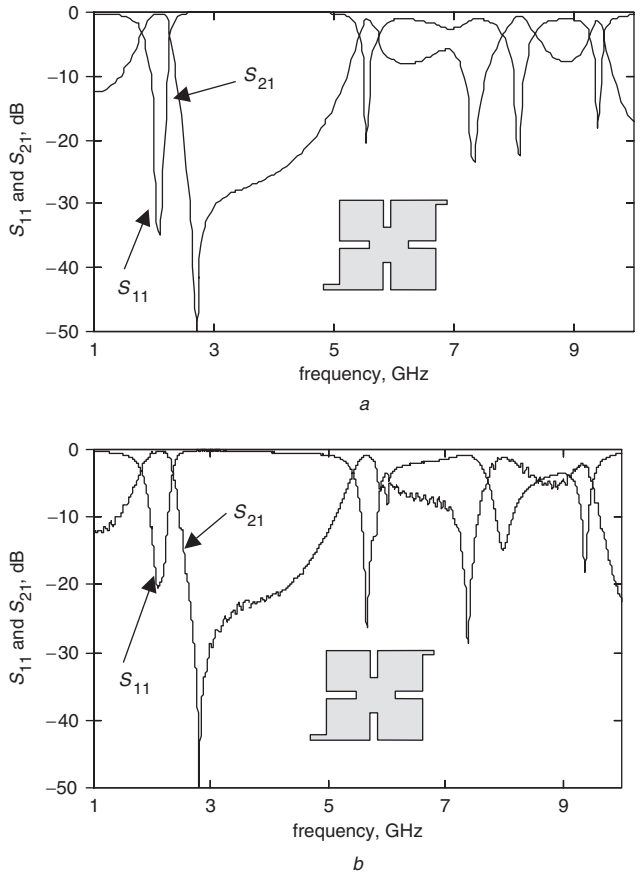

Fig. 9 *Simulations (based on IE3D) and experimental results of a one-element two-pole filter*
a Simulation results
b Experimental results

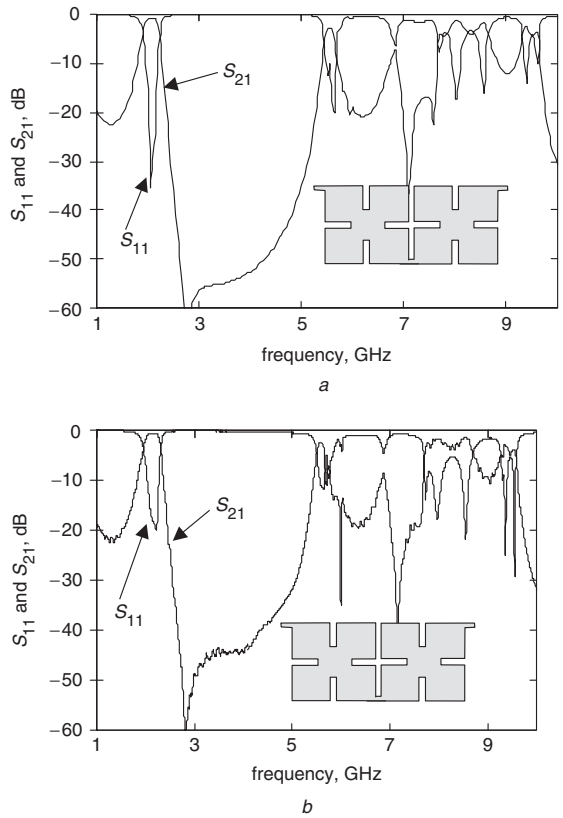

Fig. 10 *Simulations (based on IE3D) and experimental results of two cascaded elements four-pole filter*
a Simulation results
b Experimental results

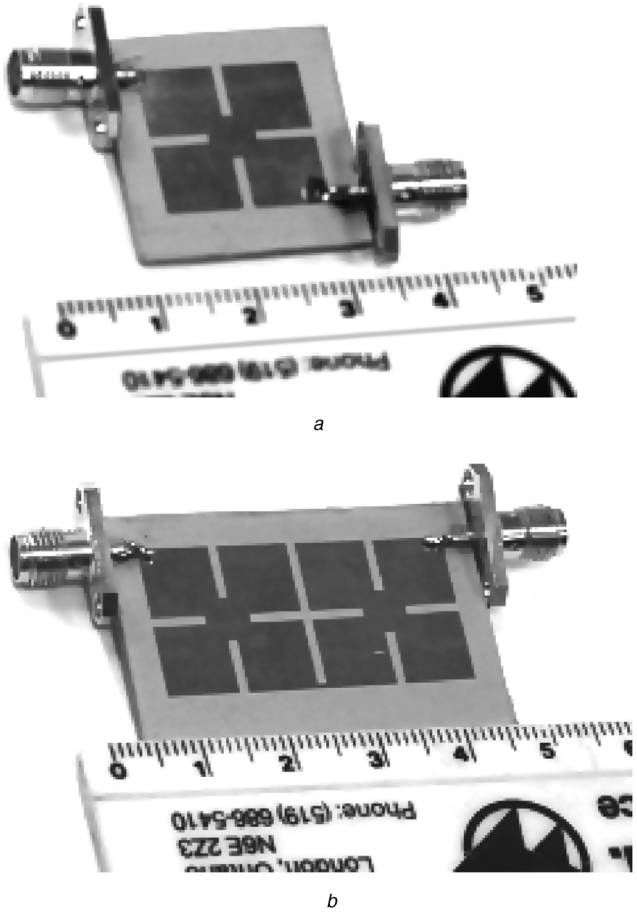

Fig. 11 *Photographs of the fabricated filters*
a One-element two-pole filter
b Two-element four-pole filter

5 Conclusions

A new nondegenerate dual-mode patch resonator for filter applications has been proposed. The new structure uses a square patch resonator with four slots etched in symmetrical form. An important size reduction compared to conventional degenerate dual-mode square patch has been achieved without significantly sacrificing the filter performance. Design flexibility for fractional bandwidths from about 5% to more than 25% has been demonstrated. A 13% bandpass filter has been designed at 2.15 GHz on Duroid substrate with $\varepsilon_r = 10.2$ and $h = 0.635$ mm. Good agreement between theoretical and experimental results is observed.

6 References

1 Wolff, I.: 'Microsrtip bandpass filter using degenerate modes of microstrip ring resonator', *Electron. Lett.*, 1972, **8**, (12), pp. 302–303
2 Matsuo, M., Yabuki, H., and Makimoto, M.: 'Dual-mode stepped impedance ring resonator for bandpass filter applications', *IEEE Trans. Microw. Theory Tech.*, 2001, **49**, (7), pp. 1235–1240
3 Hong, J., and Lancaster, M.: 'Bandpass characteristics of new dual-mode microstrip square loop resonators', *Electron. Lett.*, 1995, **31**, (11), pp. 891–892
4 Gorur, A.: 'Description of coupling between degenerate modes of a dual-mode microstrip loop resonator using a novel perturbation arrangement and its dual-mode bandpass filter applications', *IEEE Trans. Microw. Theory Tech.*, 2004, **52**, (2), pp. 671–677
5 Hsieh, L., and Chang, K.: 'Dual-mode quasi-elliptic-function bandpass filters using ring resonators with enhanced-coupling tuning stubs', *IEEE Trans. Microw. Theory Tech.*, 2002, **50**, (5), pp. 1340–1345
6 Zhu, L., and Wu, K.: 'A joint field/circuit model of line-to-ring coupling structures and its application to the design of microstrip dual-mode filters and resonator circuits', *IEEE Trans. Microw. Theory Tech.*, 1999, **47**, (10), pp. 1938–1948

7 Curtis, J., and Fiedziuszko, S.: 'Miniature dual mode microstrip filters'. IEEE MTT-S Int. Microw. Symp. Dig., 1991, pp. 443–446
8 Mansour, R.: 'Design of superconductive multiplexers using single-mode and dual-mode filters', *IEEE Trans. Microw. Theory Tech.*, 1994, **42**, (7), pp. 1411–1418
9 Hong, J., and Li, S.: 'Theory and experiment of dual-mode microstrip triangular patch resonators and filters', *IEEE Trans. Microw. Theory Tech.*, 2004, **52**, (4), pp. 1237–1243
10 Zhu, L., Wecowski, P., and Wu, K.: 'New planar dual-mode filter using cross-slotted patch resonator for simultaneous size and loss reduction', *IEEE Trans. Microw. Theory Tech.*, 1999, **47**, (5), pp. 650–654
11 Tan, B., Chew, S., Leong, M., and Ooi, B.: 'Modified microstrip circular patch resonator filter', *IEEE Microw. Wireless Compon. Lett.*, 2002, **12**, pp. 252–254
12 Hong, J., and Lancaster, M.: 'Microstrip filters for RF/microwave applications' (John Wiley & Sons, 2001)
13 Du, Z., Gong, K., Fu, J., and Gao, B.: 'Analysis of microstrip fractal patch antenna for multi-band communication', *Electron. Lett.*, 2001, **37**, pp. 805–806
14 Semouchkina, E., Cao, W., Mittra, R., and Lanagan, M.: 'Effect of feeding symmetry on resonances in patch and capacitor structures'. IEEE MTT-S Int. Microw. Symp. Dig., 2001, pp. 486–489